

## OPTICAL BEAM QUALITY IN FREE-ELECTRON LASERS\*

P.A. Sprangle<sup>#</sup>, Naval Research Laboratory, Washington, DC, 20375, U.S.A.

H.P. Freund, Science Applications International Corp., McLean, VA 22102, U.S.A.

J. Peñano, Naval Research Laboratory, Washington, DC, 20375, U.S.A.

B. Hafizi, Icarus Research Inc., P.O. Box 30780, Bethesda, MD 20824-0780, U.S.A.

### Abstract

It is widely known that the mode quality of the output of free-electron lasers (FELs) is near the diffraction limit. In this paper, we analyze the optical mode quality in FELs using the  $M^2$  parameter, which is an optical analogue of the emittance for particle beams and measures the divergence of the optical mode. For a perfect Gaussian beam  $M^2 = 1$  and increases as the mode quality deteriorates (*i.e.*, the divergence angle and the higher order mode content increase). Thus, the optical mode is often described as  $M^2$  times diffraction limited in the far field. We show how  $M^2$  may be calculated in two ways: (1) by a direct integration over the transverse mode structure, and (2) by allowing the mode to expand beyond the wiggler and analyzing the divergence. We then simulate a forthcoming experiment at Brookhaven National Laboratory using the MEDUSA simulation code and show that  $M^2$ , as expected, is near unity at saturation.

### INTRODUCTION

It is widely known that the mode quality of the output of free-electron lasers (FEL) is near the diffraction limit [1-3]. The question of mode quality is relevant to atmospheric propagation of high power FELs [4,5]. Numerical analysis has shown that the mode content in oscillators is predominantly in the TEM<sub>00</sub> mode by solution of the paraxial wave equation for a fixed electron beam profile and the subsequent decomposition into Gaussian optical modes [1]. The optical mode quality was observed in the Los Alamos FEL oscillator [2,3] where the mode was shown to be near the diffraction limit. The mode quality in this experiment was characterized by a measurement of the Strehl ratio, which is defined as the ratio of the on-axis intensity at the mode waist to the intensity of a pure Gaussian mode (TEM<sub>00</sub>) with the same spot size at the lens plane. However, the Strehl ratio is difficult to determine for optical modes that differ appreciably from a Gaussian. Higher order mode content is likely to be more important in single-pass FELs, such as Master Oscillator Power Amplifiers (MOPA) or Self-Amplified Spontaneous Emission (SASE) configurations that are operated past saturation. Hence, an alternate and less ambiguous measure of beam quality is desirable.

In this paper, we quantify beam quality by means of the  $M^2$  parameter, which is an optical analog of the emittance for particle beams and provides a measure of the

divergence of the optical mode [6-8]. It is equal to unity for a perfect Gaussian beam (pure TEM<sub>00</sub>) and increases as the mode quality deteriorates (*i.e.*, the divergence angle of the mode and the higher order mode content increase). Thus, the optical mode is often described as  $M^2$  times diffraction limited in the far field. The  $M^2$  parameter, as well as optical mode distortion due to mirror heating was measured in the FEL oscillator experiment at Thomas Jefferson National Accelerator Facility [9]. This experiment produced average powers in excess of 2 kW at a wavelength of 3.1 microns. Measurements indicated beam quality near the diffraction limit with  $M^2 = 1.1$  at the output mirror for powers up to about 350 W. As the power increased beyond 350 W,  $M^2$  increased and reached values of about 2 for powers of 500 W. However, much of the increase in  $M^2$  that occurred at higher power increased was attributed to mirror distortions and not the wave-particle interaction in the FEL. As a result, the mode quality may be improved in high-power oscillators using mirrors that compensate for distortions. Note that the mode quality in high-power amplifiers is governed solely by the FEL interaction.

In this paper we determine  $M^2$  in two ways: (1) by a direct integration over the transverse mode structure, and (2) by allowing the mode to expand beyond the wiggler and analyzing the mode divergence. This is discussed in Sec. II. In Sec. III we study  $M^2$  in FEL amplifiers using the MEDUSA simulation code [10,11] and then simulate a forthcoming experiment at the Source Development Laboratory at Brookhaven National Laboratory. A summary and discussion is given in Sec. IV.

### THE $M^2$ PARAMETER

A perfect Gaussian beam experiences parabolic expansion in which the spot size increases on either side of the waist via [12]

$$w^2(z) = w_0^2 + \frac{\lambda^2}{\pi^2 w_0^2} (z - z_0)^2, \quad (1)$$

where  $w(z)$  is the spot size,  $w_0$  is the minimum spot size (*i.e.*, at the waist),  $\lambda$  is the wavelength, and  $z_0$  is the location of the waist. Note that the Rayleigh range is given by  $z_R = \pi w_0^2 / \lambda$  so that  $w^2(z_0 \pm z_R) = 2w_0^2$  and the optical mode area increases by a factor of two over the course of the Rayleigh range. The asymptotic diffraction angle is given by  $\tan \theta_D = \lambda / \pi w_0 = w_0 / z_R$ . Since the waist size is, typically, much less than the Rayleigh range, this means that  $\theta_D \approx \lambda / \pi w_0$ .

\*Work supported by the JTO and ONR

<sup>#</sup>sprangle@ppd.nrl.navy.mil

A similar expression describing parabolic expansion also holds for a more general optical beam that includes higher order modes and can be written as [6-8]

$$W^2(z) = W_0^2 + M^4 \frac{\lambda^2}{\pi^2 W_0^2} (z - z_0)^2, \quad (2)$$

where the upper case  $W_0$  corresponds to the average waist size for the overall optical beam, and

$$W^2(z) = 2 \frac{\iint dx dy r^2 I(x, y, z)}{\iint dx dy I(x, y, z)}, \quad (3)$$

denotes the spot size of the overall optical mode where  $I(x, y, z)$  is the average (over a wave period) intensity. Observe that in the limit of a purely Gaussian optical beam,  $W(z) = w(z)$  and  $M^2 = 1$ . As such  $M^2 (\geq 1)$  is a measure of the optical beam quality and is the optical analogue of the emittance for particle beams. Note also that this definition of  $M^2$  can unambiguously deal with optical modes that differ markedly from a pure Gaussian, unlike the definition of the Strehl ratio. This asymptotic divergence angle  $\theta_D$  is given by

$$\tan \theta_D = M^2 \frac{\lambda}{\pi W_0}, \quad (4)$$

so that  $\theta_D \approx M^2 \lambda / \pi W_0$  for small divergence angles. This is shown schematically in Fig. 1.

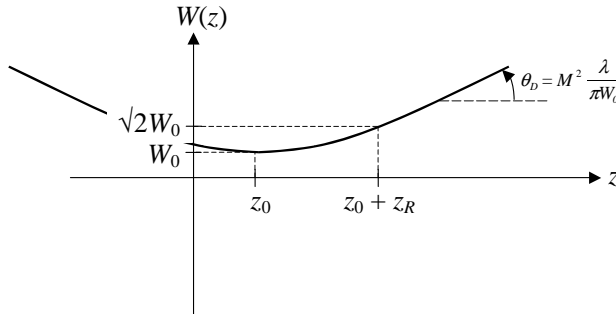


Figure 1: Schematic illustration of parabolic mode expansion

In general, the optical mode may be expressed as a superposition of Gauss-Hermite modes and we can write

$$\delta \mathbf{A}(\mathbf{x}, t) = \hat{\mathbf{e}}_{x, l, n} \sum_{l, n} e_{l, n}(x, y) [\delta A_{l, n}^{(1)} \cos \varphi(x, t) + \delta A_{l, n}^{(2)} \sin \varphi(x, t)], \quad (5)$$

where  $e_{l, n}(x, y) = \exp[-r^2/w(z)^2] H_l[\sqrt{2}x/w(z)] H_n[\sqrt{2}y/w(z)]$ ,  $H_l$  is the Hermite polynomial of order  $l$ ,  $\varphi(\mathbf{x}, t) = k_0 z - \omega t + \alpha(z)r^2/w(z)^2$  for wavenumber  $k_0 (= \omega/c)$  and angular frequency  $\omega$  and  $\alpha(z)$  describes the curvature of the phase front. For propagation *in vacuo*, the amplitudes  $\delta A^{(1,2)}$  are constant,  $\varphi$  is the overall phase, and the spot size and curvature vary as  $w(z) = w_0 [1 + (z - z_0)^2/z_R^2]^{1/2}$  and  $\alpha(z) = (z - z_0)/z_R$ . However, the optical mode in a FEL is both amplified and guided by the interaction with the electron beam so that the amplitudes, spot size and curvature will vary in a more complex way along the length of the wiggler. Nevertheless, it may be shown that the overall spot size is given in terms of this representation by

$$W^2(z) = w^2(z) \frac{S_2}{S_1}. \quad (6)$$

where

$$S_1 = \sum_{l, n} 2^{l+n} l! n! \delta A_{l, n}^2, \quad (7)$$

$$S_2 = \sum_{l, n} 2^{l+n} l! n! [(l+n+1) \delta A_{l, n}^2 + 2(l+1)(l+2) (\delta A_{l, n}^{(1)} \delta A_{l+2, n}^{(1)} + \delta A_{l, n}^{(2)} \delta A_{l+2, n}^{(2)}) + 2(n+1)(n+2) (\delta A_{l, n}^{(1)} \delta A_{l, n+2}^{(1)} + \delta A_{l, n}^{(2)} \delta A_{l, n+2}^{(2)})], \quad (8)$$

and  $\delta A_{l, n}^2 = \delta A_{l, n}^{(1)2} + \delta A_{l, n}^{(2)2}$ . Observe that  $S_1 = S_2$  for a pure Gaussian Mode (TEM<sub>00</sub>) and we recover  $W(z) = w(z)$ .

We now discuss the calculation of the  $M^2$  parameter. If we express the overall field in the form  $\delta \mathbf{A}(\mathbf{x}, t) = A(\mathbf{x}) \hat{\mathbf{e}}_x \cos[k_0 z - \omega t + \theta(\mathbf{x})]$ , then it may be shown that

$$M^2 = \left[ \iint dx dy I \right]^{-1} \times \left\{ \left( \iint dx dy r^2 I \right) \left( \iint dx dy \left[ \left( \frac{\partial I^{1/2}}{\partial r} \right)^2 + I \left( \frac{\partial \theta}{\partial r} \right)^2 \right] \right) - \left( \iint dx dy I \frac{\partial \theta}{\partial r} \right)^2 \right\}^{1/2}, \quad (9)$$

where the intensity is  $I = (\omega k_0 / 8\pi) A^2$ . As a result, it can be shown that

$$M^2 = \frac{W^2(z)}{w^2(z)} \left[ \frac{2w^2(z)}{W^2(z)} - 1 - \frac{S_3}{S_2} + \frac{S_4}{S_2} \right]^{1/2}, \quad (10)$$

where

$$S_3 = 2 \sum_{l, n} 2^{l+n} l! n! [(l+1)(l+2) (\delta A_{l, n}^{(2)} \delta A_{l+2, n}^{(1)} - \delta A_{l, n}^{(1)} \delta A_{l+2, n}^{(2)}) + (n+1)(n+2) (\delta A_{l, n+2}^{(2)} \delta A_{l, n}^{(1)} - \delta A_{l, n}^{(2)} \delta A_{l, n+2}^{(1)})], \quad (11)$$

$$S_4 = \sum_{l, l', n, n'} F_{l, l', n, n'} (\delta A_{l, n}^{(1)} \delta A_{l', n'}^{(1)} - \delta A_{l, n}^{(2)} \delta A_{l', n'}^{(2)}), \quad (12)$$

and

$$F_{l, l', n, n'} = \frac{1}{\pi} \int_0^{2\pi} d\theta \int_0^\infty d\rho \rho \exp(-\rho^2) \times [\cos \theta H_l'(\rho \cos \theta) H_n(\rho \sin \theta) + \sin \theta H_l(\rho \cos \theta) H_n'(\rho \sin \theta)] \times [\cos \theta H_{l'}'(\rho \cos \theta) H_{n'}(\rho \sin \theta) + \sin \theta H_{l'}(\rho \cos \theta) H_{n'}'(\rho \sin \theta)], \quad (13)$$

is a coefficient that depends only on the mode indices. In the limit of a purely Gaussian mode  $S_1 = S_2$ ,  $W(z) = w(z)$ , and  $S_3 = S_4 = 0$  so that Eq. (10) yields  $M^2 = 1$  as expected.

In principle, if we know the modal decomposition at the exit from the wiggler in a FEL (including the mode amplitudes, the spot size  $w$  and the curvature  $\alpha$ ), then  $M^2$  can be calculated for the output optical mode using the above method. However, if there is significant higher order mode content, then it can prove numerically arduous to evaluate the  $F_{l, l', n, n'}$  coefficients. Therefore, it is useful to have an alternate technique for obtaining  $M^2$ . One such technique makes use of the expansion of the optical mode. If the spot size is known at three different locations beyond the end of the wiggler, then the three equations  $W_i^2 = W_0^2 + M^4 \theta_0^2 (z_i - z_0)^2$  for  $i = 1-3$  can be solved for  $M^2$  where  $\theta_0 = \pi W_0 / \lambda$ . Thus,

$$M^2 = \frac{\lambda}{\pi |z_i - z_0|} \sqrt{\frac{W_i^2}{W_0^2} - 1}, \quad (14)$$

for any choice of  $i$ , where

$$z_0 = \frac{z_3 + 2z_1 + z_2}{4} + \frac{z_3 - z_2}{4} \frac{(z_3 - z_1)(W_2^2 - W_1^2) + (z_2 - z_1)(W_3^2 - W_1^2)}{(z_3 - z_1)(W_2^2 - W_1^2) - (z_2 - z_1)(W_3^2 - W_1^2)}, \quad (15)$$

and

$$W_0 = \sqrt{\frac{W_1^2 + (z_1 - z_0)^2 (z_3 - z_1)(W_2^2 - W_1^2) - (z_2 - z_1)(W_3^2 - W_1^2)}{(z_3 - z_1)(z_3 - z_2)(z_2 - z_1)}} \quad (16)$$

This technique can be applied either in experiment or simulation. When used in simulation (experiment), the optical mode must be allowed to propagate into free space and the overall spot size [(3) or (6)] must be calculated (measured) at three such points.

## NUMERICAL ANALYSIS

For simulation purposes, we use the 3-D FEL simulation code MEDUSA [10,11] which can model planar or helical wiggler geometry and treats the electromagnetic field as a superposition of Gaussian modes (Hermite or Laguerre) and uses an adaptive eigenmode algorithm called the Source-Dependent Expansion [13] to self-consistently describe the guiding of the optical mode through the wiggler and which reproduces free-space diffraction in the absence of the wiggler. The field equations are integrated simultaneously with the 3-D Lorentz force equations for an ensemble of electrons. No wiggler-average orbit approximation is used, and MEDUSA can propagate the electron beam through a complex wiggler/transport line including multiple wiggler sections, quadrupole and dipole corrector magnets, FODO lattices, and magnetic chicanes.

The example under consideration is that of a seeded amplifier experiment to be conducted at the Source Development Laboratory at Brookhaven National Laboratory [14] that will operate at a wavelength of 0.8 microns using the VISA wiggler [15]. The electron beam will have an energy of about 72.3 MeV and a peak current of 300 A. The emittance and rms energy spread are 2.0 mm-mrad and 0.01% respectively. The VISA wiggler is a Halbach design using NdFeB magnets and incorporates a FODO lattice for stronger beam focusing. The wiggler period is 1.8 cm and the maximum on-axis field strength is 7.5 kG with a field error of 0.4% and a gap of 6.0 mm. The FODO cells have a length of 24.75 cm and each quadrupole has a length of 9.0 cm and a focusing gradient of 33.3 T/m. Hence, the separation between quadrupoles is 12.375 cm. The VISA wiggler was built in segments, and the wiggler to be used in the experiment will have 110 periods of uniform field strength. The photo-cathode drive laser is also used to provide the seed for the

amplifier and can provide up to several tens of MW; however, this is larger than needed for the experiment that will use about 10-100 kW of seed power for saturation to be achieved within the length of the wiggler.

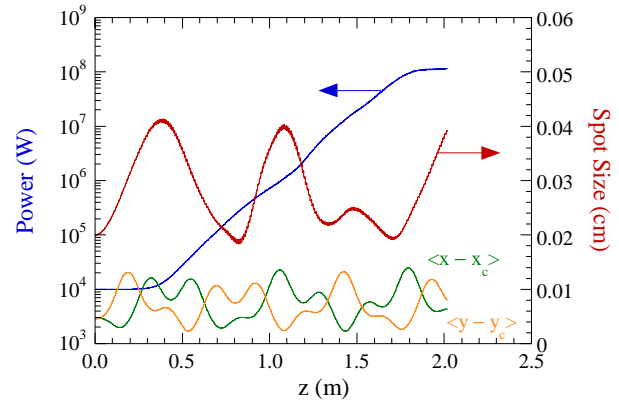


Figure 2: Evolution of the power, spot size and beam envelopes in the  $x$ - and  $y$ -directions.

The first case we consider makes use of 34 Gauss-Hermite modes and assumes a seed power of 10 kW. This yields saturation at the end of the wiggler at a power level of 115 MW. The evolution of the power, overall spot size of the optical mode, and the beam envelopes in the  $x$ - and  $y$ -directions is shown in Fig. 2. Observe that the beam is not perfectly matched into the wiggler/FODO lattice since the beam envelopes in the  $x$ - and  $y$ -directions vary in the FODO lattice and that the overall mode spot size expands and contracts with the beam envelope showing the optical guiding of the radiation; however, the guiding is not strong enough for the optical mode to follow all the variations in the beam envelope.

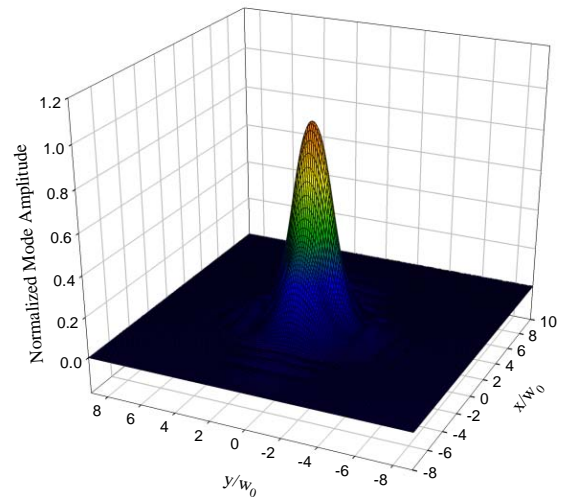


Figure 3: Transverse mode pattern at the wiggler exit for a seed power of 10 kW.

The use of 34 modes in the simulation means that very high order modes are included. Because of this the

method for calculating  $M^2$  based on integration over the transverse mode profile is numerically arduous, and we choose rather to allow the mode to propagate beyond the end of the wiggler and use the three-point solution given in Eq. (14). This can be accomplished easily in simulation simply by terminating the wiggler, after which the Source-Dependent Expansion reproduces free-space propagation when the resonant wave-particle interaction ceases. The result of this calculation shows that  $M^2 = 1.45$  for the optical mode at the wiggler exit. This is close to the diffraction limit as expected in FELs and corresponds to a near-Gaussian mode pattern as shown in a normalized transverse mode pattern in Fig. 3.

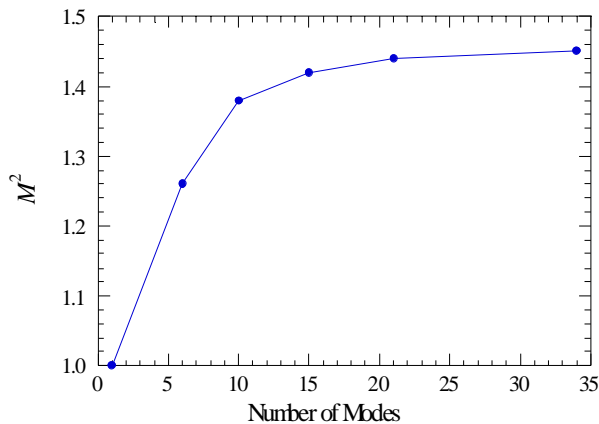


Figure 4: Variation in  $M^2$  versus the number of modes included in the simulation showing convergence after about 20 modes.

An important issue in modeling the beam quality in FELs is the convergence of the simulation with respect to the number of modes in the superposition. The number of modes required to obtain reasonable values for the saturated power is generally smaller than that required to obtain an accurate determination of the optical mode quality as measured by  $M^2$ . For example, simulation using 6 Gauss-Hermite modes also yields a saturated power of 115 MW but the exponentiation length is somewhat shorter and  $M^2 = 1.26$ . Hence, it is important to determine the number of modes required to reach convergence. This is shown in Fig. 4 for these parameters where we plot  $M^2$  versus the number of Gauss-Hermite modes in the superposition. It is clear from the figure that convergence is achieved using about 20-25 modes for  $M^2 = 1.45$ . It is important to bear in mind, however, that the number of modes required for convergence will vary with the specific parameters of interest. In particular, for optical guiding to be effective the exponentiation length must be shorter than the Rayleigh range. In general, the smaller the ratio between the exponentiation length and the Rayleigh range, the fewer the number of modes that will be needed to achieve convergence.

## SUMMARY AND DISCUSSION

In summary, we have discussed the determination of  $M^2$  in FELs by two methods. One is a direct calculation based upon the mode decomposition at any point within the wiggler, and the other relies on a three-point fit to the optical mode spot size as it propagates beyond the end of the wiggler. These techniques have been applied to an example that corresponds to an amplifier experiment at Brookhaven National Laboratory. We found that the simulation required a relatively large number of higher order modes to achieve convergence in the determination of  $M^2$ . While MEDUSA employs a Gaussian modal representation of the electromagnetic field, it is likely that this implies that alternate techniques using a transverse field solver will require a relatively fine mesh to achieve the same result. Further, the results indicate that the beam quality to be expected is near-diffraction limited when the wiggler length is comparable to the saturation length.

## REFERENCES

- [1] D.C. Qiumby and J. Slater, IEEE J. Quantum Electron. QE-19 (1983) 800.
- [2] B.E. Newnam *et al.*, IEEE J. Quantum Electron. QE-21 (1985) 867.
- [3] B.E. Newnam *et al.*, Nucl. Instrum. Meth. A237 (1985) 187.
- [4] P.A. Sprangle, B. Hafizi, and J.R. Peñano, IEEE J. Quantum Electron. 40 (2004) 1739.
- [5] P.A. Sprangle, J.R. Peñano, and B. Hafizi, J. Directed Energy (to appear 2006).
- [6] A.E. Siegman, Proc. Soc. Photo-Opt. Instrum. Eng. 1224 (1990) 2.
- [7] T.F. Johnson, Jr., Laser Focus World 26 (1990) 173.
- [8] A.E. Siegman, IEEE J. Quantum Electron. 27 (1991) 1146.
- [9] S.V. Benson, J. Gubeli, and M. Shinn, Nucl. Instrum. Meth. A483 (2002) 434.
- [10] H.P. Freund *et al.*, IEEE J. Quantum Electron. 36 (2000) 275.
- [11] H.P. Freund, Phys. Rev. ST-AB 8 (2005) 110701.
- [12] A.E. Siegman, *Lasers* (University Science Books, Mill Valley, CA, 1986).
- [13] P.A. Sprangle, A. Ting, and C.M. Tang, Phys. Rev. A 36 (1987) 2773.
- [14] T. Watanbe *et al.*, "Design study of a compact megawatt class FEL amplifier based on the VISA undulator," presented at the 27<sup>th</sup> Int'l. Free Electron Laser Conference, Stanford, CA, 21-26 August 2005.
- [15] R. Carr *et al.*, Phys. Rev. ST-AB, 4 (2001) 122402.